Acta Geodyn. Geomater., Vol. 22, No. 2 (218), 137–150, 2025
DOI: 10.13168/AGG.2025.0010
journal homepage: https://www.irsm.cas.cz/acta

ORIGINAL PAPER

GNSS-BASED VELOCITY ESTIMATION USING LINEAR AND MACHINE LEARNING APPROACHES, WITH STRAIN ANALYSIS IN THE BALTIC SEA REGION

Mehmet EREN *

Department of Geomatic Engineering, Yildiz Technical University, Istanbul, Türkiye

**Corresponding author's e-mail:* meren@yildiz.edu.tr

ARTICLE INFO

Article history:
Received 31 January 2025
Accepted 15 April 2025
Available online 23 April 2025

Keywords:
GNSS Velocity Estimation
Linear Regression
Least Squares Support Vector Machines
Strain Analysis
Baltic Sea Region

ABSTRACT

In this paper, horizontal velocities are calculated using Linear Regression (LR) and Least Squares Support Vector Machines (LS-SVM) machine learning approaches to evaluate crustal deformation and tectonic stress models with the help of data provided by 42 GNSS stations along the Baltic coasts. Strain analysis for regional tectonic dynamics was performed with the help of estimated velocities based on daily GNSS observations processed in GIPSY-X software. The obtained velocity values showed statistical agreement between LR and LS-SVM at 40 stations, with LR providing lower standard deviations (±0.03–0.43 mm/year) and higher reliability for linear trends. Strain analysis reveals extensional stresses near stations MUS2, SUR4, PYRK and HAN1 due to crustal stress, while compressional stresses are observed around OSKL, KUN0, WARN and SAS2, which are probably affected by the Leba Ridge-Riga-Pskov Fault Zone. Although the optimized LS-SVM method via grid search and radial basis function kernels is advantageous for nonlinear data, it is considered more appropriate to use LR since it requires more computational resources. This study proposes the use of hybrid models (LR+LS-SVM) to capture complex deformation patterns and proves the effectiveness of LR for velocity estimation in tectonically stable regions. The findings not only provide important information for seismic hazard assessment and coastal management but also contribute to the understanding of the Baltic Sea geodynamics.

INTRODUCTION

Comprehension of the velocity fields present within coastal regions is necessary for the effective management of these areas, the environmental monitoring thereof, and the adaptation to climate change (Wöppelmann and Marcos, 2012; Jamil et al., 2024). Coastal land movement is influenced by both natural and anthropogenic factors, leading to dynamic changes such as shoreline retreat, sediment deposition and changes in coastal landforms (Yulianto et al., 2019; Erkoç et al., 2025). These processes are particularly pronounced in regions such as the Baltic Sea, where unique geographical and hydrological features contribute to complex coastal dynamics (Baltranaitė et al., 2018; Kapsi, 2023). Addressing these challenges necessitates the utilisation of advanced tools and methodologies to facilitate accurate analysis and interpretation of coastal land movements.

GNSS is a crucial technology for measuring and analyzing crustal deformation and velocity fields, and its horizontal displacement accuracy is 2-3 times better than the vertical component (Wang et al., 2022; Erkoç and Doğan, 2023). This technology provides the necessary infrastructure for strain analysis needed to determine the temporal changes of crustal motions and to understand tectonic activities (Okazaki et al., 2021). Analyses of this nature are of particular importance in regions such as the Baltic Sea, where climate change and rising sea levels present a threat to coastal infrastructure and ecosystems (Kapsi, 2023; Ostrowski and Skaja, 2016).

In order to enhance the reliability and precision of GNSS velocity estimates, this study employed both the classical linear approximation method and an advanced machine learning algorithm, Least Squares Support Vector Machines (LS-SVM). LS-SVM, a robust extension of traditional SVM, facilitates the identification of spatial patterns in crustal deformation without relying solely on complex physical models (Najder, 2020; Yáñez-Cuadra et al., 2023; Corell and Döös, 2013; Erkoç and Doğan, 2024). Furthermore, by integrating it into strain analysis, it provides information on stress distributions and deformation dynamics, which is critical for the protection of coastal zone risks and infrastructure integrity (Carstensen et al., 2019; Grosset et al., 2023).

The Baltic Sea serves as a prime exemple for the study of these dynamics due to its vulnerability to the impacts of climate change, including relative sea-level rise and increased storm surges (Väli et al., 2013; Kotilainen et al., 2014). This research integrates GNSS measurements with strain analysis to provide a thorough examination of velocity fields and stress

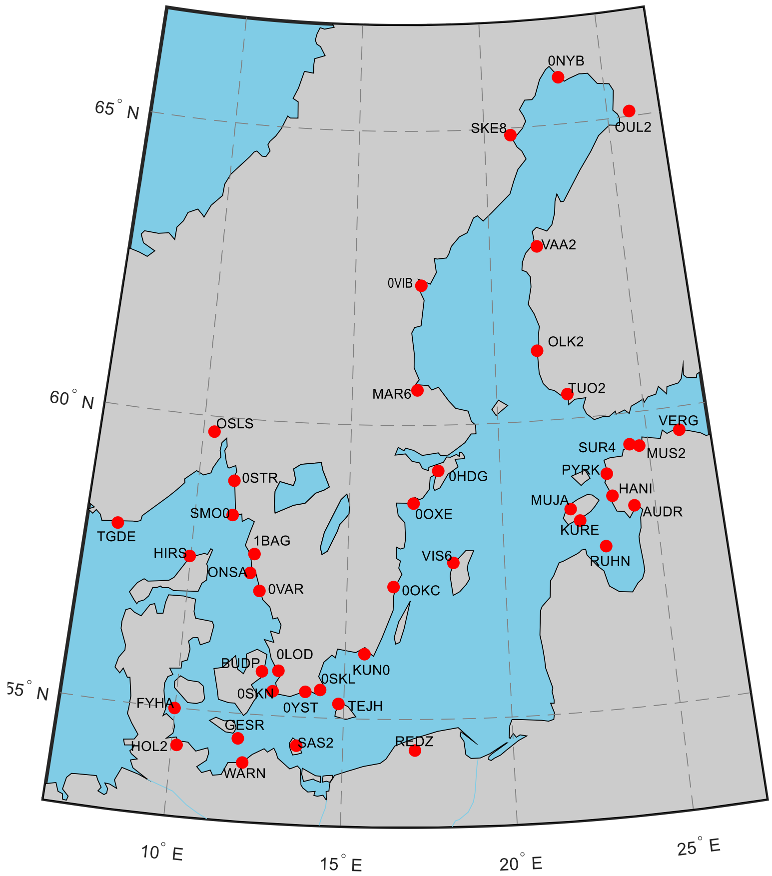

Fig. 1 Map illustrating the study area and the distribution of GNSS stations along the Baltic Sea coast.

distributions along the Baltic Sea coastline. Understanding these complex processes is of prime importance for the elaboration of sustainable coastal management strategies, supporting informed decisions, environmental monitoring, and climate adaptation efforts.

Several studies have been conducted to determine horizontal velocities using GNSS along the Baltic Sea coastline (as discussed in the referenced articles in the discussion section). However, these studies did not employ machine learning algorithms for velocity estimation. Erkoç and Doğan (2024) proved in their research that machine learning algorithms showed good performance in trend/velocity estimation. Despite these developments, a direct comparison using classical methods and machine learning approaches in GNSS velocity estimation remained limited. Building upon this foundation, this study contributes to the literature by: (a) determining horizontal velocities at 42 GNSS stations along the Baltic Sea coastline using both classical linear methods and machine learning algorithms, and (b) performing strain analysis using the velocities obtained from these stations to determine the impact of regional tectonics on the stations.

This study has two main research objectives: (1) to estimate horizontal velocities at 42 GNSS stations distributed along the Baltic Sea coastline using both classical linear methods and LS-SVM, and (2) to perform strain analysis based on the estimated velocities to assess the impact on the stations due to regional tectonics. The novelty of this study is its comparative approach to evaluate the effectiveness of traditional GNSS velocity estimation methods and machine learning techniques. The primary results of this study are the application of LS-SVM algorithm for regional-scale GNSS velocity estimation and the combined strain analysis.

DATA AND EVALUATION

STUDY AREA

The Baltic Sea is a region in Northern Europe that is notable for its geology and geography. It is considered to be a semi-enclosed brackish sea, with a noticeable salinity gradient, where the salt concentration appears to decrease from west to east (Böckmann et al., 2018; Sjöqvist et al., 2015). It comprises about 377,000 square kilometers with a considerably indented shoreline. The region is formed through dynamic interaction of tectonic, climatic, and anthropogenic processes; hence, it forms a natural laboratory to study horizontal velocity fields and deformation patterns along the coasts. Understanding these horizontal velocity fields is essential for the evaluation of coastal dynamics, relative sea-level changes, and associated risks to infrastructure and ecosystems (Fig. 1).

METHODS

The integration of GNSS-derived velocity data into strain analysis is important for the improvement of our knowledge on regional tectonic deformation and seismic hazard assessment. Long-term GNSS measurements allow the determination of strain zones by determining the accurate velocity fields of the Earth's crust. These strain zones often coincide with the highly earthquake-prone areas, since those regions that are developing at a high rate of strain build-up show more seismic vulnerability. Evidence provided by Hussain et al. (2018) and Ojo et al. (2021) suggests that the geodetic strain rate may act as proxies for seismic hazard potential and hence suggests that short-term observations are able to reflect the long-term deformation rates. This relationship points out the important contribution of the continuous monitoring GNSS does to effective seismic hazard evaluation.

In the current research, the horizontal velocities of GNSS stations are examined by two basic approaches: Linear Regression (LR) and Least Squares Support Vector Machines (LS-SVM). Preliminary examinations began with data cleansing and preparation steps, by which raw GNSS data was pre-processed to be freed from all possible disturbances from data including possible outliers or noise. The LR approach establishes a linear model for the relationship between the temporal parameters and the positional changes, which will help in analyzing the horizontal velocities. The slope of the regression line gives the estimate of the velocity of the GNSS stations; besides, the predictions are checked with actual observations based on performance metrics like Mean Squared Error and R^2. Though Linear regression is characterized by computational ease and simple implementation, it has complications in clearly formulating the nonlinear relationships, which may exist in geophysical data.

On the other hand, the LS-SVM method was utilized to address the complexities of nonlinear relationships in GNSS data. There are several key stages for the LS-SVM method: Preprocessing aims to make the data more reliable by removing noise and cleaning outliers to increase the reliability of the data. Then, a suitable kernel function is selected. For this analysis, the Radial Basis Function (RBF) kernel is chosen. Then, the parameters of the kernel and the regularization term are optimized by systematic grid search for cross-validation. This process is important for selecting appropriate values of the model parameters, especially the regularisation parameter (γ) and the kernel parameter (σ), which significantly affect model accuracy and performance (Van Gestel et al., 2001). It has been observed that the parameter σ can significantly affect the RMSE, suggesting that a precisely chosen σ can improve performance (Boscolo et al., 2022). In addition, the values of the LS-SVM parameters γ and σ (hyperparameters) have been optimised. These have been used in different areas of application with effective grid search methodologies (Syarif et al., 2016). This process involves tuning the parameters within a defined range, fitting LS-SVM on several subsamples of the data, and validating the model on the remaining dataset to check the parameter tuning that keeps the prediction error as minimum as possible. After establishing the parameters of the model, the LS-SVM model is trained with the entire dataset, and the model forecasts the horizontal velocities of the GNSS stations. The model accuracy can be checked by several criteria, for instance, MSE and RMSE.

All the steps for both methodologies are provided in Table 1.

Once the station velocities are determined, the next step is to perform strain analysis. It is often done by some mathematical techniques like least-square collocation and basis function expansion. Such approaches enable the translation of discrete velocity GNSS data to continuous strain rate fields (Okazaki et al., 2021; Shen et al., 2015). For example, the least squares fitting method has been applied to model strain rates in complex geological environments, and high-resolution crustal deformation has been obtained (Arnoso et al., 2022). In addition, the Gaussian weighting function applied during the calculation of strain rates corrects local errors in velocity measurements and provides more reliable results for the obtained strain rates (Grosset et al., 2023). The steps of the strain analysis process are outlined in Table 2.

In tectonically active regions, analyses of strain ratios based on GNSS data can provide important information on the kinematics of plate movements and seismic hazards. Namely, studies have shown that strain rates can reveal regions critical for understanding fault dynamics and earthquake risks (Tretyak and Vovk, 2016; Haines and Wallace, 2020).

Strain analysis is a fundamental method for understanding deformation processes and studying the mechanical behavior of the Earth's crust in combination with stress distribution. GNSS-based strain analysis is widely used to determine tectonic plate movements, fault activity and surface deformations.

DATA ANALYSIS

A network consisting of 42 GNSS stations distributed along the coasts of the Baltic Sea was selected. Priority in the selection criteria was given to stations with at least 10 years of data, except for station SAS2, and special attention was paid to selecting stations with a minimum data gap (<4 %) at the selected stations (Table 3). The primary objective of this study is to utilize long-term data for reliable estimation of GNSS station velocities. The 24-hour datasets from these stations were downloaded from the SONEL online platform.

The GIPSY-X software, which implements the precise point positioning (PPP) strategy, was used to

Table 1 Methods used for GNSS velocity estimation and data processing strategy.

Features	Linear Regression (LR)	Least Squares Support Vector Machines (LS-SVM)
Mathematical Model	X(t) = v. t + b $v = \frac{N\Sigma(t_i \cdot X_i) - \sum t_i \sum X_i}{N\Sigma t_i^2 - (\sum ti)^2}$	$y_i = \sum_{J=1}^{N} \alpha_j K(x_j, x_i) + b$ Predictions are made using kernel functions (Duan, 2024).
Data Relationship	Assumes a linear relationship with time (Hazra and Gogtay, 2016).	Can model both linear and nonlinear relationships (Sunil, 2021).
Input Data	Time-dependent position (t, X)	Time-dependent position and more complex patterns (t, X), processed using kernel functions
Advantages	- Simple and quick calculations (Roustaei, 2024). - Simple and interpretable (Berger, 2025).	- Effectively models nonlinear relationships - Ability to cope with complex data (Si et al., 2014).
Disadvantages	- Insufficient for nonlinear data (Andrecut, 2017). - Sensitive to noise and outliers (Kallel and Ophir, 1997).	- Requires more computational resources and time (Sunil, 2021). -The need for staff specialised in domain knowledge (Sunil, 2021).
Suitability	Suitable for linear tectonic motions over time	Suitable for complex, nonlinear tectonic motions and deformation processes

Table 2 Steps involved in the strain analysis process based on displacement data from GNSS.

Step	Mathematical Expression	Description
Displacement to Strain Tensor	$\epsilon_{ij} = \frac{1}{2}(\frac{\partial u_i}{\partial x_j} + \frac{\partial u_j}{\partial x_i})$	Converts displacement gradients into strain tensor elements.
Strain Tensor Components (GNSS Data)	$\epsilon_{xx} = \frac{\partial u_x}{\partial x_x}, \epsilon_{xx} = \frac{\partial u_j}{\partial x_i}$, $\epsilon_{xy} = \frac{1}{2}(\frac{\partial u_x}{\partial y} + \frac{\partial u_y}{\partial x})$	Calculating strain tensor components from GNSS displacement data.
Volumetric Strain (Dilation)	$\epsilon_v = \epsilon_{xx} + \epsilon_{yy}$	Calculates the change in volume of the region.
Shear Strain	$\gamma = \sqrt{(\epsilon_{xx} - \epsilon_{yy}) + 4\epsilon_{xy}^2}$	Represents the change in shape of the region without volume change.
Principal Strain Values	$\lambda_1, \lambda_2 = \frac{\epsilon_{xx}+\epsilon_{yy}}{2} \pm \sqrt{\left(\frac{\epsilon_{xx}-\epsilon_{yy}}{2}\right)^2 + \epsilon_{xy}^2}$ λ_1: Maximum principal strain. λ_2: Minimum principal strain.	Determines maximum and minimum strain directions.
Principal Strain Directions	Eigenvectors of the strain tensor	Calculates the directions of principal strain corresponding to eigenvalues.
Visualization of Strain Vectors	Strain tensor eigenvalues and eigenvectors	Creates visual representations of strain using geographic information systems (GIS) or other.
Strain Mapping	Derived strain components plotted spatially	Produces maps showing tectonic faults, stress fields, or crustal deformation processes.

Table 3 Characteristics of the stations used in this study.

Station	Latitude	Longtitude	Time span	Gaps (%)	Data sources
0HDG	59.2217	17.9341	2010 - 2024	0.19	SWEPOS-LMV
0LOD	55.7669	12.9957	2002 - 2024	0.32	SWEPOS-LMV
0NYB	65.7959	23.1700	2007 - 2024	0.23	SWEPOS-LMV
0OKC	57.2519	16.4654	2013 - 2024	0.32	SWEPOS-LMV
0OXE	58.6710	17.1070	2005 - 2024	0.22	SWEPOS-LMV
0SKL	55.4749	14.2794	2005 - 2024	0.31	SWEPOS-LMV
0SKN	55.4138	12.8579	2003 - 2024	1.13	SWEPOS-LMV
0STR	58.9366	11.1813	2005 - 2024	0.14	SWEPOS-LMV
0VAR	57.1013	12.2571	2011 - 2024	0.09	(OSO) - Onsala Space Observatory
0VIB	62.3738	17.4277	2010 - 2024	0.21	SWEPOS-LMV
0YST	55.4326	13.8364	2011 - 2024	0.18	SWEPOS-LMV
1BAG	57.7209	12.0187	2013 - 2024	0.09	SWEPOS-LMV
AUDR	58.4225	24.3137	2008 - 2024	3.71	Republic of Estonian Land Board (ELB)
BUDP	55.7390	12.5000	2003 - 2024	0.82	Danish Geodata Agency
FYHA	54.9936	9.9863	2013 - 2024	0.16	DTU
GESR	54.5744	11.9229	2005 - 2024	0.45	DTU
HAN1	58.6235	23.6328	2014 - 2024	0.33	Republic of Estonian Land Board (ELB)
HIRS	57.5911	9.9675	2004 - 2024	0.41	DTU
HOL2	54.3729	10.1568	2006 - 2024	0.78	BKG
KUN0	56.1042	15.5890	2005 - 2024	0.85	SWEPOS-LMV
KURE	58.2556	22.5101	2008 - 2024	1.48	Republic of Estonian Land Board (ELB)
MAR6	60.5951	17.2585	1999 - 2024	0.24	SWEPOS-LMV
MUJA	58.4632	22.2326	2015 - 2024	0.95	Republic of Estonian Land Board (ELB)
MUS2	59.4211	24.6980	2012 - 2024	2.41	Republic of Estonian Land Board (ELB)
OLK2	61.1910	21.5060	2014 - 2024	0.83	
ONSA	57.3953	11.9255	1996 - 2024	1.15	(OSO) - Onsala Space Observatory
OSLS	59.7370	10.3680	2000 - 2024	1.06	Kartverket
OUL2	65.0860	25.8930	2014 - 2024	2.95	NLS
PYRK	59.0066	23.5213	2014 - 2024	0.64	Republic of Estonian Land Board (ELB)
REDZ	54.4724	17.1175	2008 - 2024	3.02	ASG
RUHN	57.7823	23.2688	2014 - 2024	1.13	Republic of Estonian Land Board (ELB)
SAS2	54.5110	13.6431	2016 - 2024	0.97	BKG
SKE8	64.8792	21.0481	2015 - 2024	0.11	SWEPOS-LMV
SMO0	58.3535	11.2179	2002 - 2024	0.42	SWEPOS-LMV
SUR4	59.4636	24.3803	2011 - 2024	1.01	Republic of Estonian Land Board (ELB)
TEJH	55.2484	14.8393	2010 - 2024	2.42	DTU
TGDE	58.0073	7.5561	2009 - 2024	1.24	Kartverket
TUO2	60.4160	22.4430	2015 - 2024	0.22	NLS
VAA2	62.9610	21.7710	2014 - 2024	1.25	NLS
VERG	59.6015	26.1008	2015 - 2024	2.18	Republic of Estonian Land Board (ELB)
VIS6	57.6539	18.3674	2011 - 2024	0.20	SWEPOS-LMV
WARN	54.1698	12.1014	2004 - 2024	0.63	BKG

process the GNSS raw data. This method allows precise estimation of the coordinates of the stations in the ITRF 2020 reference frame, with precise satellite orbit and clock products. Basic error sources, including atmospheric delays (ionospheric and tropospheric), Earth orientation parameters and antenna phase center offset, were meticulously considered. On the other hand, quality control procedures such as outlier detection were applied to increase the reliability of the results.

Time series were created to analyze long-term station velocity trends with coordinated data obtained from daily solutions. Observation data covering at least nine years from each of the network stations were downloaded from the SONEL online database, which ensures consistency and high quality (see Fig. 2). This approach is in line with the methodology followed by Herring et al. (2016), who discusses the contribution of time series analysis to understanding geodynamic structure. Ren et al. (2021) noted that the trends derived from this research are one of the most important quantitative indicators of tectonic activity and, moreover, provide critical data for regional stress and seismic hazard assessment.

In this study, horizontal velocity components derived from 42 GNSS stations were separated into

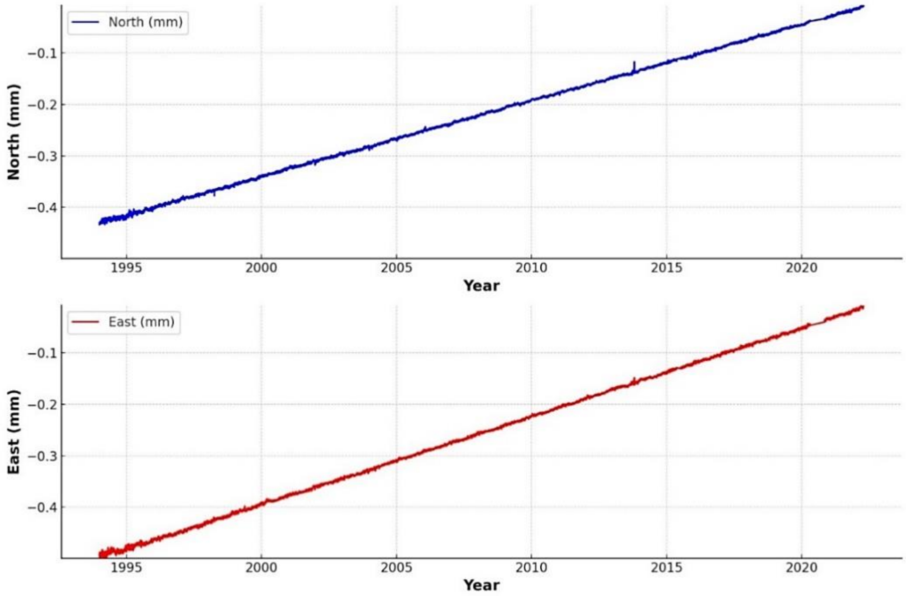

Fig. 2 Time series for the ONSA station.

their northern and eastern components, and velocity estimations were performed through time series analysis. A strain analysis was carried out using the obtained horizontal velocity components. Velocity estimation was performed based on LR and LS-SVM. The obtained horizontal components gave the necessary data for the comprehension of the spatial distribution of the deformation in the region.

The strain analysis involved computing the velocity gradient tensors, from which regional strain components were derived. These strain components are then further classified into three main types of strains: extensional strain, shear strain, and rotation. The extensional strain represents the amount of compression or extension in the area, while shear strain describes directional changes, and rotation explains the rotational movements within the area. Color scales and vector graphics have been used in this visualization of strain distribution in the whole visualization process, to get a good mapping of the compressive, extensive, and shear zones.

In addition to this, the mapping of the Strain Vector Field was also done based on this strain analysis. A map like this will give more information about deformation patterns and directions and magnitudes of the strain vectors around the region. The value of the Strain Vector Field is special in the determination of regional geodynamic processes and seismic activities.

This map, obtained because of strain analysis based on GNSS data, not only improves our understanding of tectonic movements in the region, but is also important in determining potential risk zones for seismic hazards.

RESULTS AND DISCUSSION

Monitoring horizontal velocity is important to understand the stability of the coast, which may be useful in land-use planning and mitigation strategies against coastal erosion and flooding hazards. The analyzed and predicted time series are handled using two different methods: LR and LS-SVM.

Daily GNSS observations from the stations were processed using GPSY-X software to obtain coordinate time series. The velocities and associated standard deviations derived from both methods were statistically compared using a paired t-test. The results indicated that, for 40 out of the 42 stations, there were no significant differences between the two methods at a 95% confidence level (Table 4). Consequently, the LR method was chosen for strain analysis due to its computational efficiency and consistency across the majority of stations.

The present analysis shows that the LR method is preferred for strain analysis because it provides better results for GNSS velocities along the Baltic Sea coast. In contrast, LS-SVM can be preferred in cases where nonlinear trends are more pronounced. Nevertheless, the choice of method directly affects the reliability of the results.

Detailed statistical analysis of the data (Table 4) supports the development of regional deformation models. According to the t-test results, there is no significant difference between the velocity estimates obtained from LR and LS-SVM for most stations except WARN and MAR6. The eastern component shows a significant difference of 0.91 mm/year, which is thought to be a result of sensitivity to noise or environmental factors. For station MAR6, the differences are statistically significant in both the

Table 4 t-test results for station velocities.

Station	Trend North (mm)			Trend East (mm)		
	LR	LS-SVM	$diff_{LR-SVM}$	LR	LS-SVM	$diff_{LR-SVM}$
0HDG	14.00 ± 0.12	13.76 ± 0.44	0.24 ± 0.46	18.42 ± 0.14	17.9 ± 0.59	0.52 ± 0.61
0LOD	14.90 ± 0.04	14.06 ± 0.43	0.84 ± 0.43	17.81 ± 0.09	17.09 ± 0.5	0.72 ± 0.51
0NYB	13.97 ± 0.03	13.43 ± 0.32	0.54 ± 0.32	17.40 ± 0.04	16.57 ± 0.49	0.83 ± 0.49
0OKC	14.40 ± 0.03	14.47 ± 0.98	0.07 ± 0.98	18.73 ± 0.06	18.42 ± 1.51	0.31 ± 1.51
0OXE	14.01 ± 0.14	13.47 ± 0.50	0.54 ± 0.52	18.23 ± 0.15	17.28 ± 0.72	0.95 ± 0.74
0SKL	14.61 ± 0.20	14.02 ± 0.59	0.59 ± 0.62	18.29 ± 0.27	17.42 ± 0.99	0.87 ± 1.03
0SKN	14.72 ± 0.10	14.09 ± 0.31	0.63 ± 0.33	17.93 ± 0.08	17.22 ± 0.42	0.71 ± 0.43
0STR	14.67 ± 0.12	14.22 ± 0.29	0.45 ± 0.31	15.81 ± 0.12	15.47 ± 0.41	0.34 ± 0.43
0VAR	14.99 ± 0.10	14.86 ± 0.48	0.13 ± 0.49	17.61 ± 0.11	17.54 ± 0.59	0.07 ± 0.60
0VIB	14.52 ± 0.08	14.23 ± 0.52	0.29 ± 0.53	17.01 ± 0.08	16.46 ± 0.58	0.55 ± 0.59
0YST	14.84 ± 0.04	14.89 ± 0.56	0.05 ± 0.56	18.29 ± 0.04	17.45 ± 0.80	0.84 ± 0.80
1BAG	14.99 ± 0.19	14.87 ± 0.57	0.12 ± 0.60	16.75 ± 0.17	16.90 ± 0.82	0.15 ± 0.84
AUDR	12.93 ± 0.07	12.89 ± 0.27	0.04 ± 0.28	20.15 ± 0.12	19.42 ± 0.58	0.73 ± 0.59
BUDP	15.04 ± 0.06	14.53 ± 0.39	0.51 ± 0.39	17.99 ± 0.09	17.06 ± 0.46	0.93 ± 0.47
FYHA	15.44 ± 0.25	15.10 ± 0.54	0.34 ± 0.60	17.67 ± 0.32	17.41 ± 0.85	0.26 ± 0.91
GESR	15.19 ± 0.06	14.52 ± 0.39	0.67 ± 0.39	18.33 ± 0.09	17.45 ± 0.46	0.88 ± 0.47
HAN1	13.12 ± 0.21	13.13 ± 0.63	0.01 ± 0.66	19.96 ± 0.36	20.15 ± 1.12	0.19 ± 1.18
HIRS	15.13 ± 0.19	15.14 ± 0.57	0.01 ± 0.60	16.90 ± 0.30	16.99 ± 0.91	0.09 ± 0.96
HOL2	15.34 ± 0.09	14.68 ± 0.33	0.66 ± 0.34	17.73 ± 0.08	16.97 ± 0.40	0.76 ± 0.41
KUN0	14.88 ± 0.12	14.22 ± 0.53	0.66 ± 0.54	18.98 ± 0.11	18.00 ± 0.64	0.98 ± 0.65
KURE	13.24 ± 0.07	13.32 ± 0.32	0.08 ± 0.33	20.02 ± 0.11	19.12 ± 0.52	0.90 ± 0.53
MAR6	14.17 ± 0.04	13.53 ± 0.27	0.64 ± 0.27	17.64 ± 0.05	16.66 ± 0.36	0.98 ± 0.36
MUJA	13.55 ± 0.20	13.58 ± 0.66	0.03 ± 0.69	19.66 ± 0.37	19.81 ± 1.59	0.15 ± 1.63
MUS2	12.65 ± 0.18	12.70 ± 0.51	0.05 ± 0.54	19.69 ± 0.24	19.36 ± 0.83	0.33 ± 0.86
OLK2	13.44 ± 0.06	13.54 ± 1.48	0.10 ± 1.48	19.01 ± 0.11	18.44 ± 3.09	0.57 ± 3.09
ONSA	14.83 ± 0.05	14.92 ± 0.35	0.09 ± 0.35	17.21 ± 0.05	16.43 ± 0.41	0.78 ± 0.41
OSLS	15.24 ± 0.11	15.32 ± 0.43	0.08 ± 0.44	15.83 ± 0.12	15.77 ± 0.44	0.06 ± 0.46
OUL2	13.14 ± 0.18	13.18 ± 0.54	0.04 ± 0.57	18.92 ± 0.27	19.39 ± 0.87	0.47 ± 0.91
PYRK	15.02 ± 0.20	15.16 ± 0.67	0.14 ± 0.70	18.44 ± 0.43	18.44 ± 1.07	0.00 ± 1.15
REDZ	15.36 ± 0.22	15.62 ± 0.63	0.26 ± 0.67	19.19 ± 0.24	18.67 ± 1.01	0.52 ± 1.04
RUHN	13.65 ± 0.25	13.56 ± 0.70	0.09 ± 0.74	20.46 ± 0.41	20.75 ± 1.23	0.29 ± 1.30
SAS2	14.57 ± 0.34	15.40 ± 1.28	0.05 ± 1.32	19.31 ± 0.43	19.30 ± 2.86	0.01 ± 2.89
SKE8	14.23 ± 0.09	14.27 ± 1.48	0.04 ± 1.48	17.18 ± 0.08	16.87 ± 2.19	0.31 ± 2.19
SMO0	14.84 ± 0.10	14.28 ± 0.33	0.56 ± 0.34	16.46 ± 0.07	15.65 ± 0.41	0.81 ± 0.42
SUR4	13.47 ± 0.20	13.68 ± 0.41	0.21 ± 0.46	20.02 ± 0.18	19.73 ± 0.74	0.29 ± 0.76
TEJH	15.03 ± 0.51	15.07 ± 3.06	0.04 ± 3.10	18.38 ± 0.69	18.39 ± 4.18	0.01 ± 4.24
TGDE	15.47 ± 0.07	15.13 ± 0.28	0.34 ± 0.29	16.04 ± 0.06	16.46 ± 0.30	0.42 ± 0.31
TUO2	13.16 ± 0.16	13.21 ± 0.57	0.05 ± 0.59	19.52 ± 0.28	19.27 ± 0.90	0.25 ± 0.94
VAA2	13.48 ± 0.19	13.47 ± 0.55	0.01 ± 0.58	18.42 ± 0.28	18.54 ± 0.87	0.12 ± 0.91
VERG	12.93 ± 0.22	12.96 ± 0.67	0.03 ± 0.71	20.60 ± 0.32	20.74 ± 1.94	0.14 ± 1.97
VIS6	13.92 ± 0.09	13.68 ± 0.55	0.24 ± 0.56	18.88 ± 0.12	18.02 ± 0.90	0.86 ± 0.91
WARN	15.27 ± 0.06	14.58 ± 0.34	0.69 ± 0.35	18.66 ± 0.05	17.75 ± 0.46	0.91 ± 0.46

northern (0.64 mm/year) and eastern (0.98 mm/year) components, and LS-SVM estimates lower velocities and larger uncertainties than LR.

No significant difference was found for the remaining 40 stations, indicating that LR is sufficient for use in strain analysis. LR generally provided lower standard deviation values and consistent results. The simplicity and interpretability of the LR method made it an ideal choice for velocity estimation. Such models can then be improved using more advanced machine learning methods such as LS-SVM. Hybrid models allow LR to make fast predictions, while LS-SVM improves accuracy by compensating for nonlinear components (Ren and Gao, 2011). The results show that at 40 out of 42 stations, LR and LS-SVM give statistically consistent velocities, with LR showing lower standard deviations. In particular, the largest discrepancies are observed at WARN and MAR6 stations, which is attributed to local deformation effects.

Research shows that using LS-SVM gives better results in adverse environmental conditions. For example, Dou (2023) has shown that the integrated use of LS-SVM and filtering techniques increases GNSS

Table 5 Velocities calculated by Altamimi (2020) for stations common with those used in the current study.

Station	North velocity (mm)		East velocity (mm)	
	LR	Published Data	LR	Published Data
0SKL	14.61 ± 0.20	14.7±0.09	18.29 ± 0.27	18.56±0.07
0SKN	14.72 ± 0.10	14.77±0.06	17.93 ± 0.08	18.08±0.05
0YST	14.84 ± 0.04	14.68±0.1	18.29 ± 0.04	18.43±0.08
BUDP	15.04 ± 0.06	14.94±0.03	17.99 ± 0.09	18.11±0.03
FYHA	15.44 ± 0.25	15.28±0.11	17.67 ± 0.32	17.8±0.09
HOL2	15.34 ± 0.09	15.25±0.09	17.73 ± 0.08	18.06±0.07
SAS2	14.57 ± 0.34	14.71±0.03	19.31 ± 0.43	19.03±0.03
TEJH	15.03 ± 0.51	14.84±0.28	18.38 ± 0.69	18.7±0.23
TGDE	15.47 ± 0.07	15.5±0.06	16.04 ± 0.06	16.22±0.04
WARN	15.27 ± 0.06	15.28±0.05	18.66 ± 0.05	18.64±0.04

positioning accuracy. However, as shown by Dargahi et al. (2017), LR remains a good option for horizontal velocity determination, especially in the Baltic Sea. The t-test shows that there is no statistically significant difference between the velocity values obtained from LR and the published velocity values. 10 of the stations calculated by Altamimi (2023) also gave very good agreement between the calculated and estimated velocities in the present study. This confirmed the reliability of LR (Table 5).

Kall et al. (2021) calculated the velocities of stations AUDR, KURE, and SUR4 using the Precise Point Positioning (PPP) method in a study conducted in Estonia. The results of the current study are consistent with the results of the aforementioned study and confirm the velocity estimate for these stations. Similarly, the velocities obtained by Lahtinen et al. (2021) in their studies in the Scandinavian and Baltic regions are also consistent with the findings of the current study (calculated radially). This compatibility has strengthened the reliability of the analyses to be made using these methods in regional tectonic studies.

The reliability and simplicity of the LR method strengthens its position as a preferred approach for strain analysis based on velocities estimated from GNSS. On the other hand, LS-SVM is more successful in extracting nonlinear patterns. The integration of both methods will provide more reliable results. Thus, the use of LR and LS-SVM with a hybrid approach can increase the accuracy and reliability of stress estimates by capturing both linear and nonlinear patterns in GNSS velocity estimation. Strain analysis obtained from GNSS horizontal velocities is an important tool in the fields of geodesy and tectonics and can provide important information about crustal deformation and seismic hazard. The accuracy of estimating stress ratios plays a vital role in assessing seismic risks by understanding plate interactions. The colorized strain share map visually separates compression (negative values) and extension (positive values) zones. This map shows the spatial distribution of shear stress around the Baltic Sea. Zones of intense shear deformation can be associated with fault systems/geological structures (Fig. 3). A detailed analysis of these zones can identify potential zones of tectonic stress accumulation characterized by high shear stress values.

The stress vector map indicates the direction and intensity of crustal deformation in the specified region. The direction of these vectors reflects the influence of the dominant tectonic forces; the Baltic region shows primarily north-south and east-west directional changes. The resulting pattern indicates active extensional or compressional tectonic movements in the region. Furthermore, the map highlights areas characterized by high stress vector magnitudes with localized stress accumulation and tectonic activity potential, and is associated with significant crustal deformation, especially evident along the coastal areas (see Fig. 4).

The analysis of strain rates (Exy) across the region, especially in relation to the locations of GNSS stations, provides valuable information about the tectonic processes of the region. The areas surrounding the stations MUS2, SUR4, PYRK and HAN1 are characterized by strain. The causes of this extensional behavior may be related to regional tectonic extension associated with crustal processes that stretch the Earth's crust (Yadav et al., 2021; Nucci, 2024). GNSS data from this station provide critical information for identifying current deformation mechanisms that highlight variability in the region's strain patterns and define tectonic forcing (Masson et al., 2019; Pina-Valdes et al., 2022).

In contrast, the areas close to the OSKL, KUN0, WARN, and SAS2 stations and the area between PYRK and TUO2 exhibit dominant compressional strain characteristics. This compression may indicate crustal shortening caused by local stress transfer mechanisms prevalent in the region (Métois et al., 2015; Morsut et al., 2017). The Leba Ridge-Riga-Pskov Fault Zone is identified as an important geological structure whose historical activity contributes to regional stress dynamics and influences

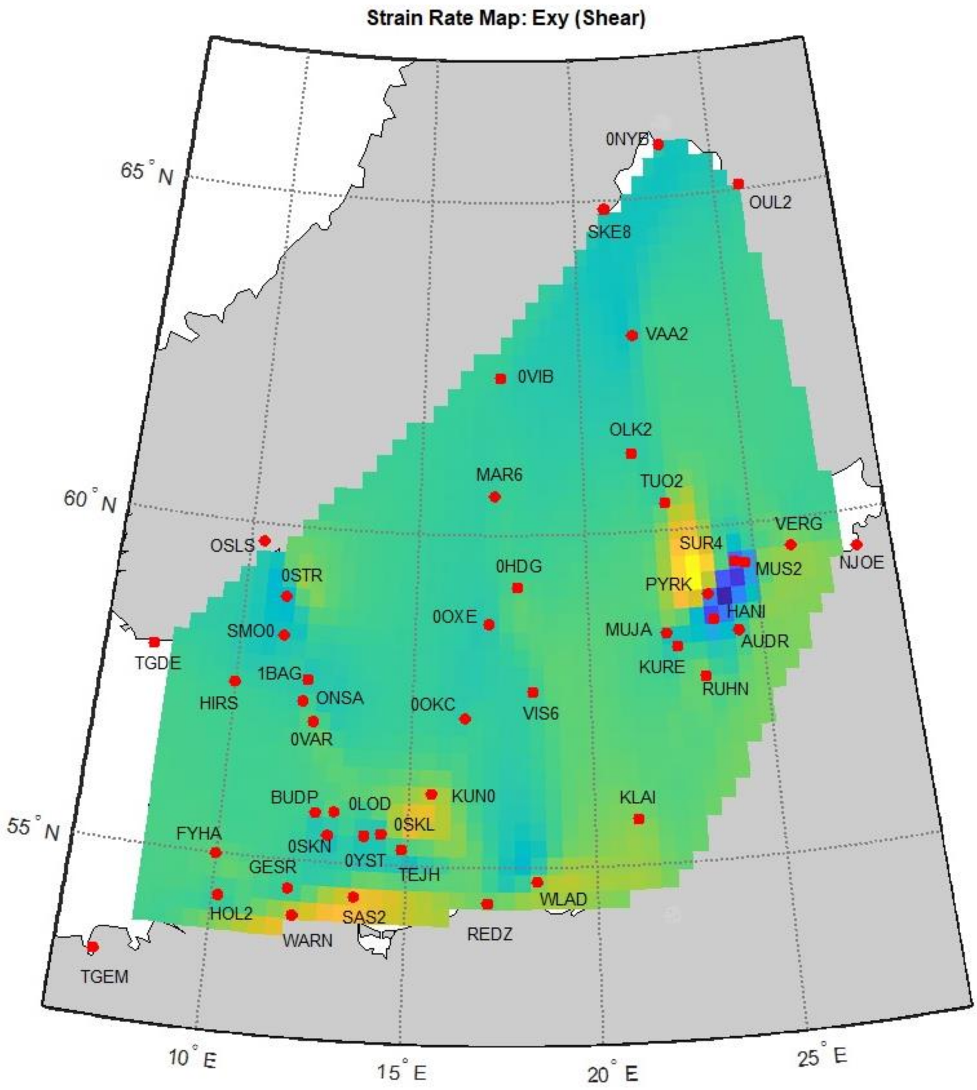

Fig. 3 This map shows the strain rate of the study area. The warmer colors on the map show higher levels of strain, while cooler colors show lower levels. The map shows where the sea is expanding and compressing.

stress distributions (Serpelloni et al., 2022; Melgar and Hayes, 2019).

Such interactions between the fault zone and crustal material surrounding it yield complicated strain patterns, which form a necessary background in understanding tectonic behavior of the area concerned. Also, worth mentioning are the sharp changes of strain around such stations as MUS2, SUR4, and PYRK-most probably an immediate reflection of stress accumulation-release processes related to activity in this fault zone. The GNSS data provides a means of quantifying these strain variations so that the associated implications for seismic hazard and tectonic stability can be estimated. Richter et al. (2014) examined the strain regimes in detail and focused on the effect of the Leba Ridge-Riga-Pskov Fault Zone in particular. This study makes a significant contribution to the full understanding of strain accumulation and transfer mechanisms. Integration of GNSS data with strain analysis has been shown to improve our understanding of tectonic processes as well as to help predict seismic events associated with these strain distributions (Li et al., 2022).

The Eastern Baltic region includes Saint Petersburg, Pskov, parts of the Novgorod and Kaliningrad regions of Russia, as well as Estonia, Latvia, Lithuania, and the southeastern parts of the

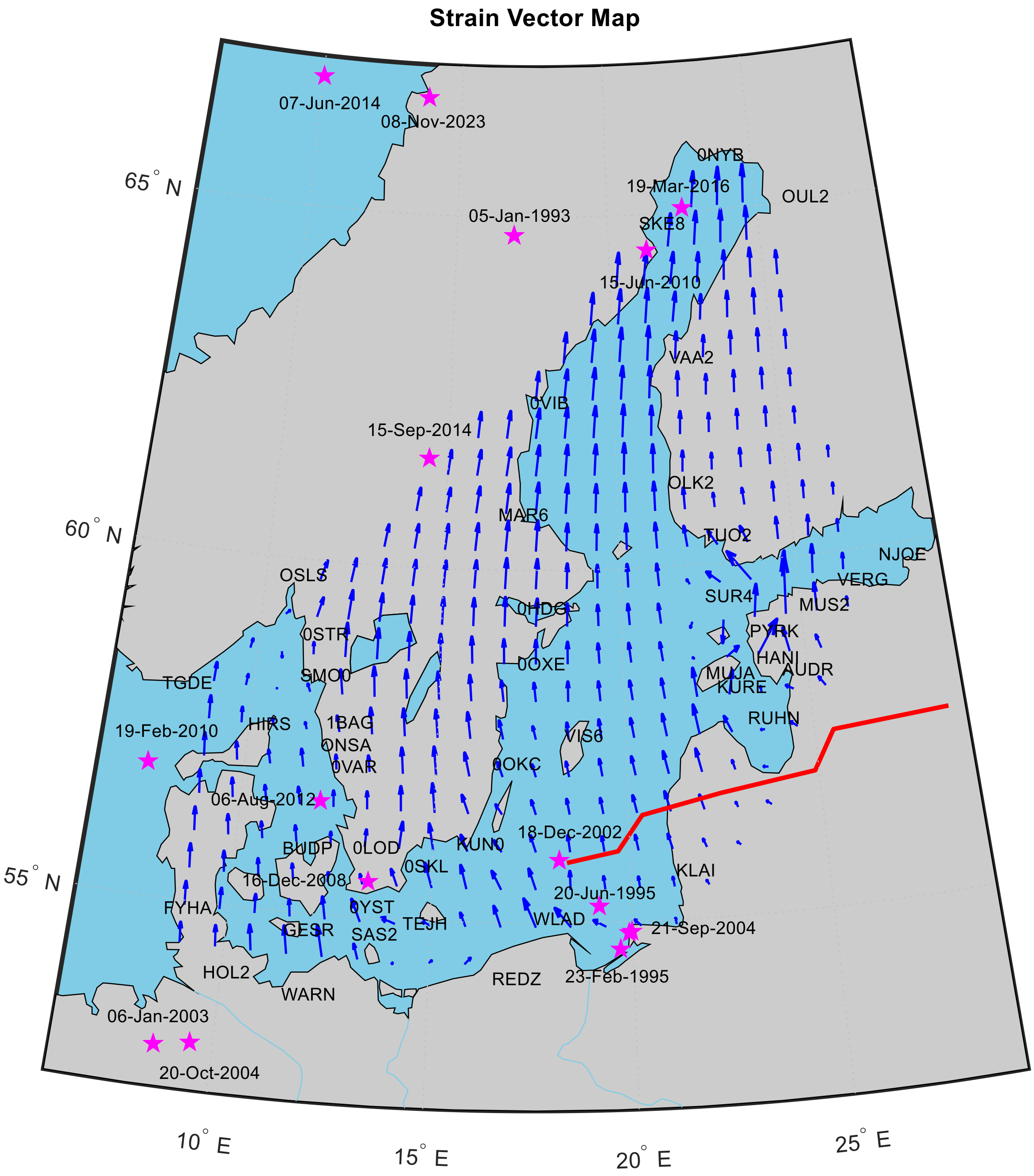

Fig. 4 Strain vector field map of the study area. Arrows show the direction and size of strain, with bigger arrows showing higher strain rates.

Baltic Sea and the Gulf of Finland. Although this region has traditionally been considered an area of low seismic activity, the Osmussaar earthquake of magnitude 4.7 on 25 October 1976 challenged this perception (Nikulins and Assinovskaya, 2018). Subsequently, the Kaliningrad earthquakes of magnitudes 5.0 and 5.2 on 21 September 2004 demonstrated that even moderate earthquakes can cause considerable damage (Nikulins and Assinovskaya, 2018). Large earthquakes in stable continental regions (SCRs) have shown that significant elastic stress can be released in geological structures located far from known fault zones. As a result, SCR earthquakes can also occur in areas with no previous seismicity and no visible surface expression of stress accumulation (Calais et al., 2016).

Consequently, continuous monitoring and analysis of GNSS data is important to improve our knowledge of hazards caused by regional geodynamics. Many studies have shown the importance of strain rates based on GNSS data in seismic hazard assessment. For example, Gülal et al. (2014) derived a relationship between geodetic strain rates and seismicity that can be used to identify areas with high seismic hazard. On the other hand, Hamling et al. (2022) provide a broad perspective on how crustal deformation adapts to tectonic forces through the analysis of long-term geological strain rates in New Zealand using GNSS data.

Spatial distribution of the GNSS station is very important for an accurate strain rate calculation. As was pointed out by Araszkiewicz et al. (2016), the sensitivity of the pattern of strain rates to GNSS station distribution underlines the necessity of a dense network, especially in such a geologically complicated region as the Baltic Sea, for precise representation of deformation dynamics. Furthermore, Karabil et al. (2018) illustrated that GNSS velocities are able to express interannual and seasonal strain variability, relating regional strain patterns to sea-level changes between the Baltic and North Sea.

These advanced GNSS horizontal velocity derivation methods, such as LS and LS-SVM techniques, produce strain analyses with important spatial variations of deformation characteristics. Such approaches have generated strain vector maps of extension and compression that are in good agreement with regional tectonic dynamics. High-strain zones, which might be related to subsidence or localized stress, are of particular interest in view of coastal hazards.

The integration of the GNSS velocity data with the most progressive analytical methods increases the reliability of strain analyses. For instance, Delen et al., (2023) discussed the advantages of integrating GNSS measurements with InSAR data to get better ground deformation results. A multi-technique approach provides a better insight into the strain distribution and its implications for regional tectonics.

CONCLUSIONS

This paper performs an extensive strain analysis supported by the calculation of horizontal velocities based on data from 42 GNSS stations distributed along the coast of the Baltic Sea and presents some important findings that will contribute to a better understanding of geodynamic and tectonic processes in this area of research.

It was found that both methods gave similar results for velocity estimation in 40 out of 42 stations, and LR provided more reliable results with lower standard deviations than LS-SVM in 2 stations. This finding shows that LR is sufficient for velocity estimation in the Baltic Sea region.

Strain analysis revealed crustal deformation patterns in the study area. Significant extensional stress regions were detected near stations MUS2, SUR4, PYRK and HAN1, indicating active crustal tension in these regions. On the other hand, the presence of compressive stresses was detected near the stations OSKL, KUN0, WARN and SAS2 and in the region between PYRK and TUO2. It is considered that these stress distributions are affected by the Leba Ridge-Riga-Pskov Fault Zone and that this has an important role in regional tectonics.

The stress vector field analysis shows dominant north-south and east-west oriented deformation patterns with significantly varying magnitudes throughout the region. Changes in the strain direction provide insight into stress accumulation processes and potential seismic hazard zones along the Baltic Sea coast.

The obtained results are in good agreement with the velocity estimates of the studies conducted in the region and the velocity estimates of the current study at the common stations, confirming the reliability of our methodology. The consistency between the studies strengthens confidence in using strain analyses based on GNSS velocities to understand regional tectonic processes.

THE RESULTS OF THIS STUDY

1. The effectiveness of LR in velocity estimation in this region has been proven and shows that simple linear methods can be used for routine monitoring of crustal deformation, providing high accuracy and low-cost solutions with simpler calculations.
2. Stress patterns determined around the Leba Ridge-Riga-Pskov Fault Zone indicate potential seismic activity in this region and are necessary to monitor for infrastructure risk assessment.
3. In urban planning, a coastal management approach that considers the spatial distribution of stress rates and the impact of areas showing crustal deformation is important.

Future research should focus on integrating GNSS horizontal velocity data with InSAR-derived surface deformation measurements to increase the resolution of stress analysis, thus facilitating better identification of local deformation patterns, especially in regions with limited GNSS station coverage. It is also proposed to develop models that take into account the relationship between glacial isostatic adjustment (GIA) and tectonic processes in the region. This will contribute to our understanding of regional geodynamics in the Baltic Sea and provide a basis for crustal deformation processes, seismic hazard assessment and sustainable coastal management strategies.

ACKNOWLEDGEMENTS

We would like to thank all data providers. GNSS data was obtained from SONEL.

REFERENCES

Altamimi, Z., Métivier, L., Rebischung, P., Rouby, H. and Collilieux, X.: 2017, ITRF2014 plate motion model. Geophys. J. Int., 209, 3, 1906–1912. DOI: 10.1093/gji/ggx136

Andrecut, M.: 2017, Randomized kernel methods for least-squares support vector machines. Int. J. Mod. Phys. C, 28, 02, 1750015. DOI: 10.1142/s0129183117500152

Araszkiewicz, A., Figurski, M. and Jarosiński, M.: 2016, Erroneous GNSS strain rate patterns and their application to investigate the tectonic credibility of GNSS velocities. Acta Geophys., 64, 5, 1412–1429. DOI: 10.1515/acgeo-2016-0057

Arnoso, J., Riccardi, U., Tammaro, U., Benavent, M., Montesinos, F. and Vélez, E.: 2022, 2D strain rate and ground deformation modelling from continuous and survey mode GNSS data in El Hierro, Canary Islands. 5th Joint International Symposium on Deformation Monitoring (JISDM 2022), Valencia. DOI: 10.4995/jisdm2022.2022.13632

Baltranaitė, E., Jurkus, E. and Povilanskas, R.: 2018, Impact of physical geographical factors on sustainable planning of south Baltic seaside resorts. Baltica, 30, 2, 119–131. DOI: 10.5200/baltica.2017.30.13

Berger, T.: 2025, On the information content of explainable artificial intelligence for quantitative approaches in finance. OR Spectrum, 47, 1, 177–203. DOI: 10.1007/s00291-024-00769-9

Boscolo, S., Nguyen, T.T., Ali, A.A., Sygletos, S. and Ellis, A.D.: 2022, Kernel adaptive filtering-based phase noise compensation for pilot-free optical phase conjugated coherent systems. Opt. Express, 30, 11, 19479–19493. DOI: 10.1364/OE.456963

Böckmann, S., Seidler, M., Schubert, H. and Kube, S.: 2018, Population genetics of two allopatric (North Sea and Baltic Sea) populations of Evadne nordmanni (Podonidae): similarities and differences. Int. Rev. Hydrobiol., 103, 3-4, 54–62. DOI: 10.1002/iroh.201701930

Calais, E., Camelbeeck, T., Stein, S., Liu, M. and Craig, T.J.: 2016, A new paradigm for large earthquakes in stable continental plate interiors. Geophys. Res. Lett., 43, 20, 10–621. DOI: 10.1002/2016GL070815

Carstensen, J., Conley, D., Almroth-Rosell, E., Asmala, E., Bonsdorff, E., Fleming-Lehtinen, V., … and Žilius, M.: 2019, Factors regulating the coastal nutrient filter in the Baltic Sea. Ambio, 49, 6, 1194–1210. DOI: 10.1007/s13280-019-01282-y

Dargahi, B., Kolluru, V. and Cvetković, V.: 2017, Multi-layered stratification in the Baltic Sea: Insight from a modeling study with reference to environmental conditions. J. Mar. Sci. Eng., 5, 1, 2. DOI: 10.3390/jmse5010002

Delen, A., Sanli, F.B., Abdikan, S., Dogan, A.H., Durdag, U.M., Ocalan, T., ... and Pepe, A.: 2023, A statistical approach for the integration of multi-temporal InSAR and GNSS-PPP ground deformation measurements. Sensors, 24, 1, 43. DOI: 10.3390/s24010043

Dou, J.: 2023, Robust GNSS positioning using unbiased finite impulse response filter. Remote Sens., 15, 18, 4528. DOI: 10.3390/rs15184528

Duan, T.: 2024, Applications of three distinct regression models in GDP prediction. Theor. Nat. Sci., 39, 1, 86–95. DOI: 10.54254/2753-8818/39/20240592

Erkoç, M.H. and Doğan, U.: 2023, Datum definition for geodetic vertical velocity field derived from GNSS observations: a case study in western and southern Turkey. Bull. Geophys. Oceanogr., 63, 1, 135–148. DOI: 10.4430/bgo00412

Erkoç, M.H. and Doğan, U.: 2024, Machine learning models applied to altimetry era tide gauge and grid altimetry data for comparative long-term trend estimation: A study from Shikoku Island, Japan. Appl. Ocean Res., 150, 104132. DOI: 10.1016/j.apor.2024.104132

Erkoç, M.H., Doğan, U., Simav, M. and Farımaz, İ.: 2025, Coastal motion at tide gauge stations along the Black Sea coast from in-situ and space-based observations. Reg. Stud. Mar. Sci., 82, 104036. DOI: 10.1016/j.rsma.2025.104036

Grosset, J., Mazzotti, S. and Vernant, P.: 2023, Glacial isostatic adjustment strain rate – stress paradox in the Western Alps, impact on active faults and seismicity. EGUsphere. DOI: 10.5194/egusphere-2023-538

Gülal, E., Tiryakioğlu, İ., Kalyoncuoğlu, Ü., Erdoğan, S., Dolmaz, M. and Elitok, Ö.: 2014, The determination of relations between statistical seismicity data and geodetic strain analysis, and the analysis of seismic hazard in Southwest Anatolia. Geomat. Nat. Hazards Risk, 7, 1, 138–155. DOI: 10.1080/19475705.2013.879743

Haines, A.J. and Wallace, L.M.: 2020, New Zealand-wide geodetic strain rates using a physics-based approach. Geophys. Res. Lett., 47, 1, e2019GL084606. DOI: 10.1029/2019gl084606

Hamling, I., Wright, T., Hreinsdóttir, S. and Wallace, L.: 2022, A snapshot of New Zealand's dynamic deformation field from Envisat InSAR and GNSS observations between 2003 and 2011. Geophys. Res. Lett., 49, 2. DOI: 10.1029/2021GL096465

Hazra, A. and Gogtay, N.: 2016, Biostatistics series module 6: Correlation and linear regression. Indian J. Dermatol., 61, 6, 593–601. DOI: 10.4103/0019-5154.193662

Herring, T., Melbourne, T., Murray, M., Floyd, M., Szeliga, W., King, R., … and Wang, L.: 2016, Plate Boundary Observatory and related networks: GPS data analysis methods and geodetic products. Rev. Geophys., 54, 4, 759–808. DOI: 10.1002/2016RG000529

Hussain, E., Wright, T., Walters, R., Bekaert, D., Lloyd, R. and Hooper, A.: 2018, Constant strain accumulation rate between major earthquakes on the North Anatolian Fault. Nat. Commun., 9, 1. DOI: 10.1038/s41467-018-03739-2

Jamil, F., Zeng, C., Ma, Y., Tun, S.H., and Ali, S.: 2024, Shear stress-strain relationships and anisotropy in silty soil: The role of principal stress rotation. Acta Geodyn. Geomater., 21, 4, 343–363. DOI: 10.13168/AGG.2024.0026

Kall, T., Kruusla, K., Liibusk, A. and Oja, T.: 2021, New 3D velocity model of Estonia from GNSS measurements. Est. J. Earth Sci., 70, 2, 107. DOI: 10.3176/earth.2021.08

Kallel, F. and Ophir, J.: 1997, A least-squares strain estimator for elastography. Ultrason. Imaging, 19, 3, 195–208. DOI: 10.1177/016173469701900303

Kapsi, I.: 2023, Sea level rise and future projections in the Baltic Sea. J. Mar. Sci. Eng., 11, 8, 1514. DOI: 10.3390/jmse11081514

Karabil, S., Zorita, E. and Hünicke, B.: 2018, Contribution of atmospheric circulation to recent off-shore sea-level variations in the Baltic Sea and the North Sea. Earth Syst. Dyn., 9, 1, 69–90. DOI: 10.5194/esd-9-69-2018

Kotilainen, A., Arppe, L., Dobosz, S., Jansen, E., Kabel, K., Karhu, J., … and Zhamoida, V.: 2014, Echoes from the past: a healthy Baltic Sea requires more effort. Ambio, 43, 1, 60–68. DOI: 10.1007/s13280-013-0477-4

Lahtinen, S., Jivall, L., Häkli, P. and Nordman, M.: 2021, Updated GNSS velocity solution in the Nordic and Baltic countries with a semi-automatic offset detection method. GPS Solut., 26, 1. DOI: 10.1007/s10291-021-01194-z

Lahtinen, S., Jivall, L., Häkli, P., Kall, T., Kollo, K., Kosenko, K., … and Nordman, M.: 2019, Densification of the ITRF2014 position and velocity solution in the Nordic and Baltic countries. GPS Solut., 23, 4. DOI: 10.1007/s10291-019-0886-3

Li, J., Yao, Y., Li, R., Yusan, S., Li, G., Freymueller, J., … and Wang, Q.: 2022, Present-day strike-slip faulting and thrusting of the Kepingtage fold-and-thrust belt in southern Tianshan: constraints from GPS observations. Geophys. Res. Lett., 49, 11. DOI: 10.1029/2022GL099105

Masson, C., Mazzotti, S., Vernant, P. and Doerflinger, E.: 2019, Extracting small deformation beyond individual station precision from dense Global Navigation Satellite System (GNSS) networks in France and Western Europe. Solid Earth, 10, 6, 1905–1920. DOI: 10.5194/se-10-1905-2019

Melgar, D. and Hayes, G.: 2019, Characterizing large earthquakes before rupture is complete. Sci. Adv., 5, 5. DOI: 10.1126/sciadv.aav2032

Métois, M., D'Agostino, N., Avallone, A., Chamot-Rooke, N., Rabaute, A., Duni, L., … and Georgiev, I.: 2015, Insights on continental collisional processes from GPS data: dynamics of the peri-Adriatic belts. J. Geophys. Res., Solid Earth, 120, 12, 8701–8719. DOI: 10.1002/2015JB012023

Morsut, F., Pivetta, T., Braitenberg, C. and Poretti, G.: 2017, Strain accumulation and release of the Gorkha, Nepal, earthquake (Mw 7.8, 25 April 2015). Pure Appl. Geophys., 175, 1, 1909–1923. DOI: 10.1007/s00024-017-1639-2

Najder, J: 2020, Automamatic detection of discontinuities in the station position time series of the reprocessed global GNSS network using Bernese GNSS Software. Acta Geodyn. Geomater., 17, 4, 439–451. DOI: 10.13168/AGG.2020.0032

Nikulins, V., and Assinovskaya, B: 2018, Seismicity of the East Baltic region after the Kaliningrad earthquakes on 21 September 2004. Baltica, 31, 1, 35–48. DOI: 10.5200/baltica.2018.31.04

Nucci, R.: 2024, Comparative analysis of methods to estimate geodetic strain rates from GNSS data in Italy. Ann. Geophys., 66, 5, DM531. DOI: 10.4401/ag-9015

Ojo, A., Kao, H., Jiang, Y., Craymer, M. and Henton, J.: 2021, Strain accumulation and release rate in Canada: implications for long-term crustal deformation and earthquake hazards. J. Geophys. Res., Solid Earth, 126, 4, e2020JB020529. DOI: 10.1029/2020JB020529

Okazaki, T., Fukahata, Y. and Nishimura, T.: 2021, Consistent estimation of strain-rate fields from GNSS velocity data using basis function expansion with ABIC. Earth Planets Space, 73, 1. DOI: 10.1186/s40623-021-01474-5

Ostrowski, R. and Skaja, M.: 2016, Influence of nearshore mining pits on hydro- and lithodynamics of a dissipative coastal zone: case study of the Hel Peninsula (Poland). Arch. Hydro-Eng. Environ. Mech., 63, 4, 237–252. DOI: 10.1515/heem-2016-0015

Pina-Valdes, J., Socquet, A., Beauval, C., Doin, M., D'Agostino, N. and Shen, Z.: 2022, 3D GNSS velocity field sheds light on the deformation mechanisms in Europe: effects of the vertical crustal motion on the distribution of seismicity. J. Geophys. Res., Solid Earth, 127, 6. DOI: 10.1029/2021JB023451

Ren, Y., Lian, L. and Wang, J.: 2021, Analysis of seismic deformation from global three-decade GNSS displacements: implications for a three-dimensional Earth GNSS velocity field. Remote Sens., 13, 17, 3369. DOI: 10.3390/rs13173369

Richter, A., Popov, S., Fritsche, M., Lukin, V., Matveev, A., Ekaykin, A., … and Dietrich, R.: 2014, Height changes over subglacial Lake Vostok, East Antarctica: insights from GNSS observations. J. Geophys. Res., Earth Surface, 119, 11, 2460–2480. DOI: 10.1002/2014JF003228

Roustaei, N.: 2024, Application and interpretation of linear-regression analysis. Med. Hypothesis Discov. Innov. Ophthalmol., 13, 3, 151–159. DOI: 10.51329/mehdiophthal1506

Serpelloni, E., Cavaliere, A., Martelli, L., Pintori, F., Anderlini, L., Borghi, A., … and Cacciaguerra, S.: 2022, Surface velocities and strain-rates in the Euro-Mediterranean region from massive GPS data processing. Front. Earth Sci., 10. DOI: 10.3389/feart.2022.907897

Shen, Z., Wang, M., Zeng, Y. and Wang, F.: 2015, Optimal interpolation of spatially discretized geodetic data. Bull. Seismol. Soc. Am., 105, 4, 2117–2127. DOI: 10.1785/0120140247

Si, G., Shi, J., Guo, Z. and Zhao, W.: 2014, Efficient sparse least squares support vector machines for regression. Proc. 33rd Chinese Control Conference, Nanjing 2014, 5173–5178. DOI: 10.1109/ChiCC.2014.6895821

Sjöqvist, C., Godhe, A., Jonsson, P., Sundqvist, L. and Kremp, A.: 2015, Local adaptation and oceanographic connectivity patterns explain genetic differentiation of a marine diatom across the North Sea–Baltic Sea salinity gradient. Mol. Ecol., 24, 11, 2871–2885. DOI: 10.1111/mec.13208

Sunil, A.: 2021, Stock price prediction using LSTM model and Dash. Int. J. Res. Appl. Sci. Eng. Technol., 9, 1, 142–144. DOI: 10.22214/ijraset.2021.32760

Syarif, I., Prugel-Bennett, A. and Wills, G.: 2016, SVM parameter optimization using grid search and genetic algorithm to improve classification performance. TELKOMNIKA (Telecom. Comp. Elect. and Cont.), 14, 4, 1502–1509. DOI: 10.12928/telkomnika.v14i4.3956

Tretyak, K. and Vovk, A.: 2016, Differentation of the rotational movements of the European continent´s Earth crust. Acta Geodyn. Geomater., 13, 1, 5–18. DOI: 10.13168/AGG.2015.0046

Väli, G., Meier, H. and Elken, J.: 2013, Simulated halocline variability in the Baltic Sea and its impact on hypoxia during 1961–2007. J. Geophys. Res., Oceans, 118, 12, 6982–7000. DOI: 10.1002/2013JC009192

Van Gestel, T., Suykens, J.A.K., Baestaens, D.-E., Lambrechts, A., Lanckriet, G., Vandaele, B., … Vandewalle, J.: 2001, Financial time series prediction using least squares support vector machines within the evidence framework. IEEE Trans. Neural Netw., 12, 4, 809–821. DOI: 10.1109/72.935093

Wang, S., Li, J., Chen, J. and Hu, X.: 2022, On the improvement of mass load inversion with GNSS horizontal deformation: a synthetic study in Central China. J. Geophys. Res., Solid Earth, 127, 10. DOI: 10.1029/2021JB023696

Wöppelmann, G. and Marcos, M.: 2012, Coastal sea level rise in southern Europe and the nonclimate contribution of vertical land motion. J. Geophys. Res., Oceans, 117, C1. DOI: 10.1029/2011JC007469

Yadav, A., Kannaujiya, S., Ray, P., Yadav, R. and Gautam, P.: 2021, Estimation of crustal deformation parameters and strain build-up in northwest Himalaya using GNSS data measurements. Contrib. Geophys. Geod., 51, 3, 225–243. DOI: 10.31577/congeo.2021.51.3.2

Yáñez-Cuadra, V., Moreno, M., Ortega-Culaciati, F., Donoso, F., Baez, J. and Tassara, A.: 2023, Mosaicking andean morphostructure and seismic cycle crustal deformation patterns using GNSS velocities and machine learning. Front. Earth Sci., 11. DOI: 10.3389/feart.2023.1096238

Yulianto, F., Suwarsono, S., Maulana, T. and Khomarudin, M.: 2019, The dynamics of shoreline change analysis based on the integration of remote sensing and geographic information system (GIS) techniques in Pekalongan coastal area, Central Java, Indonesia. J. Degrad. Min. Lands Manage., 6, 3, 1789–1782. DOI: 10.15243/jdmlm.2019.063.1789